dermal cells producing IFN-γ and IL-12 per ear in pre-exposed mice was 1.02×10^5 and 3.2×10^4, which are 9- and 15-fold greater than in naïve mice, respectively. Langerhans cells and keratinocytes are important sources of IL-12 in the skin (*24, 26*), and each of the major epidermal populations has been shown to produce IFN-γ (*24, 27, 28*). The early and increased production of IFN-γ and IL-12 in the inoculation site may activate infected macrophages for killing during the initial establishment of infection and may also promote a more rapid and polarized *Leishmania*-specific T helper cell type 1 response.

The strong DTH response elicited at the inoculation site in mice previously exposed to sand fly bites conferred immunity against *L. major* infection that was as potent as any achieved by the combination of parasite antigens and adjuvants used to date. These findings imply that the exposure history of individuals to the bites of uninfected sand flies influences the incidence and severity of cutaneous leishmaniasis and that for this and possibly other vector-borne diseases, salivary antigens might be effective components of vaccines directed against transmitted pathogens.

References and Notes

1. J. M. C. Ribeiro, *Exp. Parasitol.* **69**, 104 (1989).
2. S. K. Wikel, *BioScience* **49**, 311 (1999).
3. R. Beach, G. Kiilu, J. Leeuwenburg, *Am. J. Trop. Med. Hyg.* **34**, 278 (1985).
4. E. Pozio, M. Maroli, L. Gradoni, M. Gramiccia, *Trans. R. Soc. Trop. Med. Hyg.* **79**, 524 (1985).
5. R. Lainson, R. D. Ward, J. J. Shaw, *Nature* **266**, 628 (1977).
6. R. Killick-Kendrick, A. J. Leaney, P. D. Ready, D. H. Molyneux, *Proc. R. Soc. London* **196**, 105 (1977).
7. P. G. Lawyer, D. G. Young, *J. Med. Entomol.* **24**, 458 (1987).
8. P. G. Lawyer *et al.*, *Trans. R. Soc. Trop. Med. Hyg.* **84**, 229 (1990).
9. Female BALB/c and C57BL/6 mice, aged 8 to 12 weeks, were purchased from the Division of Cancer Treatment, National Cancer Institute, Frederick, MD. IL-4–deficient mice, generated from an C57BL/6 embryonic stem cell line, were provided by N. Noben-Trauth.
10. Two- to 4-day-old *P. papatasi* females were obtained from a colony initiated from field specimens collected in Saudi Arabia. Flies were infected by artificial feeding on a chick membrane at 37°C. The bloodmeal consisted of heparinized mouse blood drawn intracardially from BALB/c mice, plus penicillin (100 U/ml) and streptomycin (100 μg/ml) to which 2×10^6 to 3×10^6 *L. major* amastigotes (MHOM/IL80/Friedlin) clone V1 were added. The amastigotes had been harvested from BALB/c footpads and cryopreserved in liquid nitrogen. Blood-fed flies were separated the following day and kept in an incubator at 25° to 26°C and 85 to 95% relative humidity. They were fed on a solution of 50% sucrose, 5% albumin, and sterile water through soaked cotton balls. The majority of infected flies showed a heavy parasite load (mean number, 60,000), a blocked stomodeal valve, and a high proportion of metacyclic promastigotes (≥30%) on days 14 to 15 after infection, when they were used for transmission. Flies were placed in plastic vials (volume, 3 drams; height, 4.8 cm; diameter, 1.8 cm) covered at one end with a 0.25-mm nylon mesh. Mice were anesthetized by intraperitoneal injection of 200 μl of ketamine hydrochloride (20 mg/ml) (Phoenix Pharmaceuticals, St. Joseph, MO). Individual ears of anesthetized mice were pressed flat against the mesh surface with specially designed clamps that held the vial and ear in place between support arms adapted at the ends with a flat rubber surface. The mice were also restrained by tape across the tail and back. Five or 10 infected flies were used per ear, and they were allowed to feed for 2 to 3 hours in the dark, after which time each fly was examined for blood.
11. The flies used for the pre-exposure of mice to the bites of uninfected sand flies were emergent females, left without sugar or water, and used the following day. For pre-exposure, flies were left to feed on both ears (10 to 15 flies per ear) for a period of 30 to 40 minutes in the dark, after which time at least five flies per ear became fully engorged with blood. Mice were exposed twice to uninfected flies at biweekly intervals.
12. M. Brossard, S. K. Wikel, *Med. Vet. Entomol.* **11**, 270 (1997).
13. S. K. Wikel, *Int. J. Parasitol.* **29**, 851 (1999).
14. P. Willadsen, F. Jongejan, *Parasitol. Today* **15**, 258 (1999).
15. Web table 1 and Web fig. 1 are available at *Science* Online at www.sciencemag.org/cgi/content/full/290/5495/1351/DC 1.
16. Y. Belkaid *et al.*, *J. Exp. Med.* **188**, 1941 (1998).
17. R. G. Titus, J. M. Ribeiro, *Science* **239**, 1306 (1988).
18. Y. Belkaid *et al.*, *J. Immunol.* **165**, 969 (2000).
19. M. L. Mbow, J. A. Bleyenberg, L. R. Hall, R. G. Titus, *J. Immunol.* **161**, 5571 (1998).
20. M. L. Cross, M. S. Cupp, E. W. Cupp, F. B. Ramberg, F. J. Enriquez, *J. Med. Entomol.* **30**, 725 (1993).
21. N. S. Zeidner, S. Higgs, C. M. Happ, B. J. Beaty, B. R. Miller, *Parasite Immunol.* **21**, 35 (1999).
22. Complete ears were fixed in 10% phosphate-buffered formalin and embedded in paraffin. Thin sections (5 μm) were stained with hematoxylin and eosin. The transverse section showing the greatest thickness was measured with an ocular micrometer.
23. To obtain cells from a homogenate of the entire ear dermis, the sheets were separated and placed dermal side down in Dulbecco's modified Eagle's medium (DMEM) containing penicillin (100 U/ml), streptomycin (100 μg/ml), and collagenase A (1 mg/ml). After a 2-hour incubation at 37°C, the dermal sheets were cut into small pieces, filtered through a 70-μm nylon cell strainer, and rinsed twice in RPMI containing 20% fetal bovine serum, penicillin (100 U/ml), and streptomycin (100 μg/ml). The first rinse included 0.05% deoxyribonuclease. The leukocyte subpopulations were identified by characteristic size and granulosity, combined with two-color analysis as previously described (*16, 29*). For each sample, 10,000 cells were analyzed with CELLQuest software (Becton Dickinson, San Jose, CA).
24. A. Takashima, P. R. Bergstresser, *Semin. Immunol.* **8**, 333 (1996).
25. Epidermal cells were isolated from unbitten ears and from ears 6 hours after exposure to infected *P. papatasi*, according to a method recently described (*16*). Briefly, the epidermis was separated from the dermis after a 30-min incubation of the dermal sheets in DMEM and 0.5 to 0.1% trypsin at 37°C. The epidermal cells were collected through a 70-μm cell strainer, distributed in six-well plates, and incubated in Brefeldin A (Sigma) for 6 hours at 37°C. The cells were fixed in 4% paraformaldehyde and incubated in a permeabilization buffer consisting of antibody to Fc receptor in phosphate-buffered saline containing 10% normal mouse serum and 0.1% saponin. The cells were then washed and incubated with a battery of antibodies to cytokine and their isotype controls, each directly conjugated to R-phycoerythrin (Pharmingen), as specified previously (*16*). The stained cells were fixed again in 1% paraformaldehyde and washed, and for each sample, 100,000 cells were analyzed with CELLQuest software.
26. K. Kang *et al.*, *J. Immunol.* **156**, 1402 (1996).
27. A. Fayyazi *et al.*, *Arch. Dermatol. Res.* **291**, 485 (1999).
28. M. Sugaya, K. Nakamura, K. Tamaki, *J. Invest. Dermatol.* **113**, 350 (1999).
29. Y. Belkaid, H. Jouin, G. Milon, *J. Immunol. Methods* **199**, 5 (1996).

30. We thank J. Ribeiro and A. Sher for their critical evaluation of the manuscript.

7 June 2000; accepted 10 October 2000

Regulation of Antigen-Specific CD8$^+$ T Cell Homeostasis by Perforin and Interferon-γ

Vladimir P. Badovinac,[1] Amy R. Tvinnereim,[1] John T. Harty[1,2]*

T cell memory depends on factors that regulate expansion and death of these cells after antigenic stimulation. Mice deficient in perforin and interferon-γ (IFN-γ) exhibited increased expansion, altered immunodominance, and decreased death of antigen-specific CD8$^+$ T cells after infection with an attenuated strain of *Listeria monocytogenes*, which was cleared from these mice. Expansion of CD8$^+$ T cells was controlled by perforin, whereas IFN-γ regulated immunodominance and the death phase. Thus, perforin and IFN-γ regulate distinct elements of CD8$^+$ T cell homeostasis independently of their role as antimicrobial effector molecules.

In response to infection, CD8$^+$ T cells expand and differentiate into effector cells, which mediate pathogen clearance through perforin-dependent cytolysis or elaboration of IFN-γ or tumor necrosis factor (TNF) (*1*). The magnitude of expansion varies, depending on the infection, and reproducible hierarchies of immunodominance are observed in pathogen-specific CD8$^+$ T cell responses. After pathogen clearance, antigen-specific (Ag-specific) CD8$^+$ T cells undergo a reproducible death phase in which 80 to 90% of the expanded CD8$^+$ T cells are eliminated, irrespective of the magnitude of the initial expansion. The remaining Ag-specific memory CD8$^+$ T

[1]Department of Microbiology and [2]Interdisciplinary Graduate Program in Immunology, University of Iowa, Iowa City, IA 52242, USA.

*To whom correspondence should be addressed. E-mail: john-harty@uiowa.edu

cells are maintained throughout the life of the host. The factors controlling the expansion, immunodominance hierarchies, and the death phase of $CD8^+$ T cells remain undefined. Perforin and IFN-γ might regulate $CD8^+$ T cell homeostasis through their role in resistance to infection (*1*) or through pathways that are independent of their antimicrobial effector functions (*2*). We addressed this issue by analyzing Ag-specific $CD8^+$ T cell homeostasis in mice with perforin and/or IFN-γ deficiency.

$CD8^+$ T cell responses were elicited in wild-type and gene knockout (KO) mice by infection with an attenuated ActA-deficient *Listeria monocytogenes* (LM) strain (DP-L1942) (*3*) that elicits protective $CD8^+$ T cell–mediated resistance in IFN-γ–deficient mice (*4*). At 7 days post infection (p.i.) of BALB/c (H-2^d MHC) wild-type mice, $CD8^+$ T cells specific for the dominant $LLO_{91\text{-}99}$ and subdominant $p60_{217\text{-}225}$ epitopes of LM represented 1/50 and 1/256, respectively, of splenic $CD8^+$ T cells (Fig. 1, A and B) as detected by intracellular staining (ICS) for TNF. This technique detects the majority of Ag-specific $CD8^+$ T cells identified by ICS for IFN-γ (*5*, *6*) or by tetrameric major histocompatibility complex (MHC) class I–peptide staining (*7*). Similar results were reported after infection of wild-type mice with virulent LM (*8*–*10*). Expansion of Ag-specific $CD8^+$ T cells in wild-type mice is followed by a death phase, which is essentially complete by 14 days p.i. (Fig. 1B). The resulting memory levels of Ag-specific $CD8^+$ T cells were maintained for at least 60 days p.i.

Infection of H-2^d MHC perforin/IFN-γ–deficient (PKO/GKO) mice (*11*) with DP-L1942 resulted in altered homeostasis of Ag-specific $CD8^+$ T cells (Figs. 1 and 2). Expansion of $LLO_{91\text{-}99}$- and $p60_{217\text{-}225}$-specific $CD8^+$ T cells at day 7 p.i was significantly increased to 1/11 and 1/16, respectively, of splenic $CD8^+$ T cells (Fig. 1, A and B). PKO/GKO mice contain 9-fold ($LLO_{91\text{-}99}$) and 33-fold ($p60_{217\text{-}225}$) greater total Ag-specific $CD8^+$ T cells as a result of increased spleen size (*12*). Thus, $CD8^+$ T cell expansion is aberrant in PKO/GKO mice. In addition, the nearly equivalent expansion of $LLO_{91\text{-}99}$- and $p60_{217\text{-}225}$-specific $CD8^+$ T cells in PKO/GKO mice resulted in a dramatic alteration of the immunodominance hierarchy normally observed in wild-type mice, where $LLO_{91\text{-}99}$ responses were four- to six-fold higher than $p60_{217\text{-}225}$ responses (Fig. 1, A and B).

The death phase of $CD8^+$ T cells is also abnormal in PKO/GKO mice (Figs. 1B and 2D). No significant decrease in Ag-specific $CD8^+$ T cells is observed at 14 days p.i. of PKO/GKO mice, a time at which the death phase (~75% loss) is essentially complete in

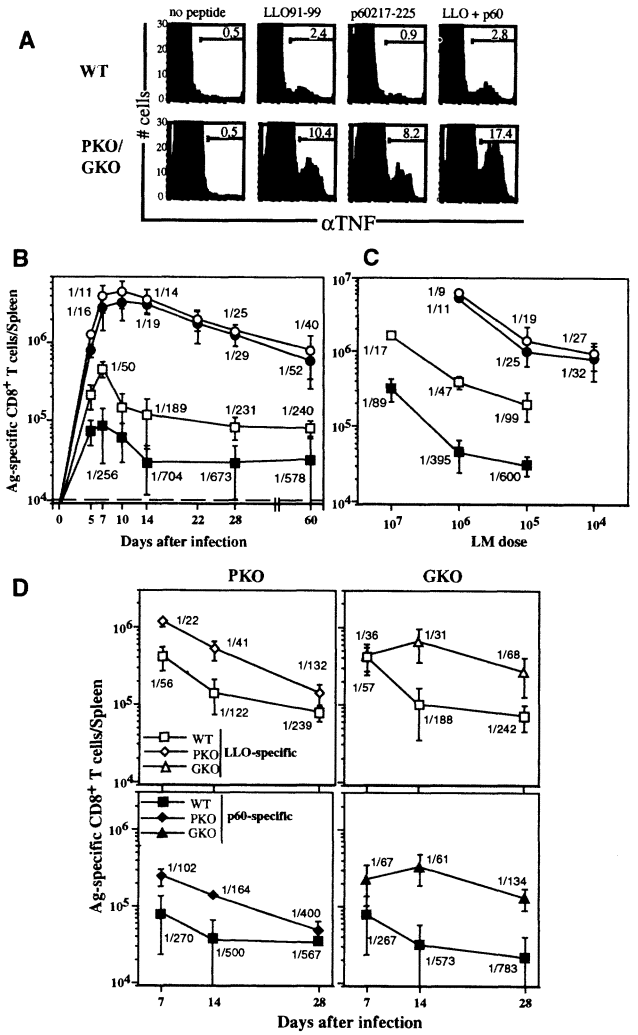

Fig. 1. Kinetics of Ag-specific $CD8^+$ T cell responses after LM infection in wild-type (WT) and perforin- and/or IFN-γ–deficient mice. Wild-type and PKO/GKO mice were infected with $1.3 \times 10^6 \pm 0.4$ LM strain DP-L1942 (*37*) and Ag-specific $CD8^+$ T cells in the spleen were measured by ICS for TNF (*38*). (**A**) Data are from representative mice at day 7 p.i. Numbers represent the percent of TNF^+ $CD8^+$ T cells in the absence or presence of $LLO_{91\text{-}99}$ (*39*) and/or $p60_{217\text{-}225}$ (*40*) peptides. (**B**) Total number per spleen (mean ± SD) and frequencies of Ag-specific $CD8^+$ T cells obtained from 4 to 15 wild-type or PKO/GKO mice per time point. (□), WT-LLO; (■), WT-p60; (○), PKO/GKO-LLO; (●), PKO/GKO-p60. Dashed line represents limit of detection. (**C**) Total number per spleen (mean ± SD) and frequencies of Ag-specific $CD8^+$ T cells obtained from three wild-type or PKO/GKO mice per group at day 7 p.i. with the indicated dose of DP-L1942. Symbols are as in (B). (**D**) Wild-type, PKO, and GKO mice were infected with $1.2 \times 10^6 \pm 0.2$ DP-L1942, and the frequency and total number (mean ± SD) of $LLO_{91\text{-}99}$- (top row) or $p60_{217\text{-}225}$-specific (bottom row) $CD8^+$ T cells in the spleen was determined by ICS for TNF at the indicated days. Data was obtained from 3 to 12 mice per time point.

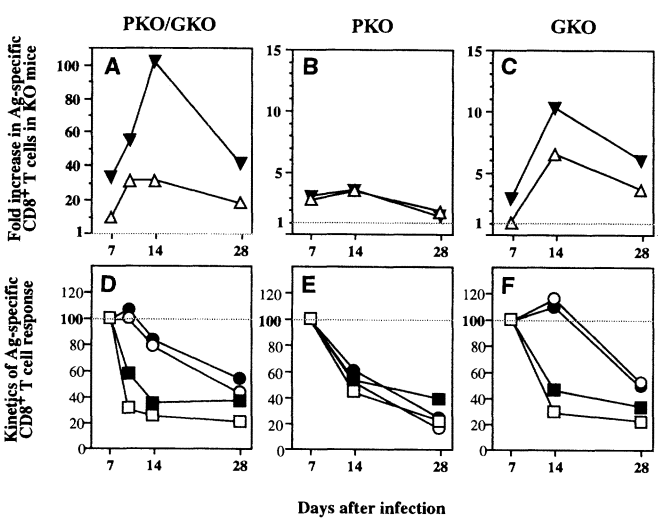

Fig. 2. Immunodominance and Ag-specific $CD8^+$ T cell death in PKO/GKO, PKO, GKO, and wild-type mice. (**A** through **C**) Increase in $LLO_{91\text{-}99}$- and $p60_{217;225}$-specific $CD8^+$ T cells in PKO/GKO, PKO, and GKO mice compared with wild-type mice at the indicated days after infection. The total number of $LLO_{91\text{-}99}$- and $p60_{217\text{-}225}$-specific $CD8^+$ T cells per spleen of the indicated KO mouse was divided by the total number of epitope-specific $CD8^+$ T cells per spleen of wild-type mice. (△), LLO-KO/WT; (▼), p60-KO/WT. (**D** through **F**) Normalized death of $LLO_{91\text{-}99}$- and $p60_{217\text{-}225}$-specific $CD8^+$ T cells in PKO/GKO, PKO, and GKO mice compared with wild-type mice at the indicated time points after LM infection. At the peak of primary response (day 7 p.i.), the frequency of $LLO_{91\text{-}99}$- or $p60_{217\text{-}225}$-specific $CD8^+$ T cells are presented as 100%. (□), WT-LLO; (■), WT-p60; (○), KO-LLO; (●), KO-p60.

wild-type mice. At 28 days p.i., the frequency and total numbers of Ag-specific $CD8^+$ T cells in PKO/GKO mice are less than twofold reduced compared with the levels at day 14 p.i. Thus, the rate of Ag-specific $CD8^+$ T cell death is dramatically reduced in PKO/GKO mice (Fig. 2D). Together, these data show that Ag-specific $CD8^+$ T cell expansion, immunodominance, and death are disrupted in PKO/GKO mice.

PKO/GKO mice harbor more organisms than wild-type mice at 2 days p.i. (*12*), which could contribute to the increased expansion of Ag-specific $CD8^+$ T cells. However, the ~10-fold increase in bacterial numbers does not appear sufficient to cause the ~1000-fold shift in the dose response of $CD8^+$ T cell expansion in PKO/GKO compared with wild-type mice (Fig. 1C). Furthermore, the altered immunodominance hierarchy in PKO/GKO mice does not result from increased antigen load because it is observed at all doses of infection, whereas the normal immunodominance hierarchy in wild-type mice is preserved at all doses (Fig. 1C). Lastly, PKO/GKO mice clear infection by 10 days p.i. (*12*). Thus, the aberrant death phase of Ag-specific $CD8^+$ T cells does not result from persistent infection. These data suggest that the impact of perforin and IFN-γ on $CD8^+$ T cell homeostasis is distinct from their roles in clearance of infection.

Perforin is a critical component of the cytolytic effector pathways of $CD8^+$ T cells in resistance to infection (*13*). In addition, perforin plays a role in exhaustion of Ag-specific $CD8^+$ T cells after lymphocytic choriomeningitis virus (LCMV) infection (*2*, *14*). To determine the contribution of perforin deficiency to altered $CD8^+$ T cell homeostasis, H-2^d MHC perforin-deficient (PKO) (*15*) and wild-type mice were infected with DP-L1942 and Ag-specific $CD8^+$ T cell responses were analyzed. Expansion of both LLO_{91-99}- and $p60_{217-225}$-specific $CD8^+$ T cells was increased three- to fourfold in PKO mice compared with wild-type mice (Figs. 1D and 2B). However, the total number and frequency of LLO_{91-99}-specific $CD8^+$ T cells remained four- to fivefold greater than the $p60_{217-225}$ response (Fig. 1D), and the normal immunodominance hierarchy was preserved in PKO mice. In addition, $CD8^+$ T cells in PKO mice exhibited a relatively normal death phase (Figs. 1D and 2E). Clearance of DP-L1942 infection was indistinguishable between PKO and wild-type mice (*12*). Furthermore, immunization of PKO mice with peptide-coated dendritic cells (DC) resulted in a threefold higher expansion of LLO_{91-99}-specific $CD8^+$ T cells compared with wild-type mice (Fig. 3). Thus, perforin regulates $CD8^+$ T cell expansion independently of its role as an effector molecule in resistance to infection.

IFN-γ has multiple roles in response to infection, ranging from up-regulation of molecules involved in antigen presentation (*16*) to activation of microbicidal macrophages (*17*). Infection of H-2^d MHC IFN-γ–deficient (GKO) mice (*4*) with DP-L1942 resulted in similar frequencies and total numbers of LLO_{91-99}-specific $CD8^+$ T cells at day 7 compared with wild-type mice (Fig. 1D). In contrast, the frequency and total number of $CD8^+$ T cells specific for $p60_{217-225}$ was higher in GKO mice (fourfold and threefold, respectively) compared with wild-type mice, indicating that normal immunodominance hierarchies are not maintained in GKO mice (Figs. 1D and 2C). In contrast to wild-type mice, the frequencies and total number (Figs. 1D and 2F) of $CD8^+$ T cells specific for either epitope did not decrease at 14 days p.i. for GKO mice and remained elevated at 28 days p.i. This result occurred despite clearance of the infection by day 10 (*12*). Thus, IFN-γ deficiency had little impact on $CD8^+$ T cell expansion against the dominant LLO_{91-99} epitope but resulted in altered immunodominance hierarchies and decreased death rate of Ag-specific $CD8^+$ T cells.

We next examined $CD8^+$ T cell homeostasis after infection with LCMV, which elicits vigorous $CD8^+$ T cell priming against the dominant $NP_{118-126}$ epitope, representing >50% of splenic $CD8^+$ T cells at day 8 p.i. for wild-type mice (Fig. 4A) (*18*). In wild-type mice, virus is cleared and a rapid death phase ensues in which the majority of Ag-specific $CD8^+$ T cells are eliminated by day 15 p.i. In contrast, PKO mice do not clear the infection and eventually die (*2*, *14*); however, LCMV is cleared from GKO mice by 12 days p.i., and these GKO mice mount $CD8^+$ T cell responses against the $NP_{118-126}$ epitope (*19*). Thus, we examined the death phase of $NP_{118-126}$-specific $CD8^+$ T cells in wild-type and GKO mice after LCMV infection (Fig. 4). Both wild-type and GKO mice

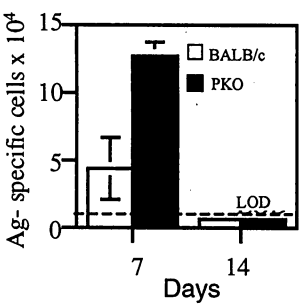

Fig. 3. Expansion of Ag-specific $CD8^+$ T cells in wild-type and PKO mice in the absence of infection. LLO_{91-99}-coated (2×10^5) DC (*41*) were injected intravenously into wild-type or PKO mice. Four wild-type and three PKO mice were analyzed on day 7 for LLO_{91-99}-specific $CD8^+$ T cells by ICS for IFN-γ. Two mice from each group were analyzed at day 14. LOD, limit of detection, 5×10^3 Ag-specific $CD8^+$ T cells per spleen. The percent of $CD8^+$ T cells and spleen sizes were similar between groups.

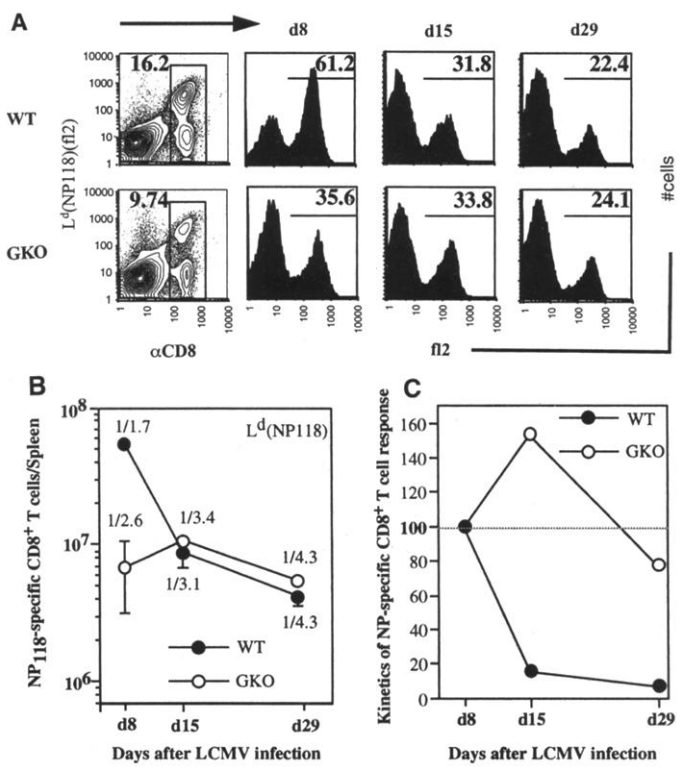

Fig. 4. Kinetic analysis of $NP_{118-126}$-specific $CD8^+$ T cells during LCMV infection. Wild-type and GKO mice were infected with 5×10^5 plaque-forming units (PFU) of LCMV strain Armstrong (*10*), and the frequency of $NP_{118-126}$-specific $CD8^+$ T cells in the spleen was determined by MHC class I tetramer $L^d(NP_{118})$ (*18*) staining. **(A)** Frequency of $NP_{118-126}$-specific $CD8^+$ T cells from representative mice at day 8, 15, and 29 p.i. Numbers represent the percent of $CD8^+$ T cells that stain with $L^d(NP_{118})$. Frequency of $CD8^+/L^d(NP_{118})^+$ in naïve mice was <1%. **(B)** Total number (mean ± SD) and frequencies of $NP_{118-126}$-specific $CD8^+$ T cells per spleen from three mice per time point. **(C)** Normalized death of $NP_{118-126}$-specific $CD8^+$ T cells in GKO mice and wild-type mice. At day 8 p.i., the total number of $NP_{118-126}$-specific $CD8^+$ T cells per spleen is presented as 100%.

made a vigorous $NP_{118-126}$-specific $CD8^+$ T cell response as detected by MHC class I tetramer staining at 8 days p.i., although the response of wild-type mice was higher than that of GKO mice. Similar results were obtained with ICS for TNF (*7*). These data suggest that IFN-γ contributes to the massive expansion of $CD8^+$ T cells after LCMV infection of wild-type mice, perhaps through its ability to promote optimal antigen presentation (*20*). Strikingly, the substantial death phase observed in wild-type mice did not occur in GKO mice (Fig. 4, A through C). The total number of Ag-specific cells per spleen in GKO mice was only slightly reduced at day 29, a time at which wild-type mice contain <10% of the levels obtained at the peak of expansion. Consistent with previous reports, we could detect no LCMV in blood samples obtained at 12 days p.i. of wild-type or GKO mice. Thus, IFN-γ also contributes to the death phase of Ag-specific $CD8^+$ T cells after LCMV infection.

Our results demonstrate that perforin and IFN-γ regulate distinct elements of Ag-specific $CD8^+$ T cell homeostasis. Perforin deficiency could enhance $CD8^+$ T cell expansion through decreased killing of antigen presenting cells (APC) (*21*, *22*), resulting in prolonged Ag-display and the stimulation of additional naïve precursor cells. Alternatively, perforin may act directly on Ag-specific $CD8^+$ T cells by controlling the balance between division and death during the expansion phase. The possibility that $CD8^+$ T cells become sensitive to their own perforin was originally suggested after demonstration that perforin-deficient $CD8^+$ T cells fail to undergo exhaustive deletion after LCMV infection (*2*).

Immunodominance in $CD8^+$ T cell responses is a well-recognized but poorly understood phenomenon that may be controlled by the available T cell receptor (TCR) repertoire, strength of peptide-MHC binding, antigen processing, and/or antigen levels (*23*). Extensive studies of these parameters in the LM infection model suggested that immunodominance may be a consequence of the available TCR repertoire (*9*, *24–26*). However, it is not clear how the absence of IFN-γ would impact the development of the naïve T cell repertoire. One possibility is that the proteosome changes associated with IFN-γ signaling (*16*) actually decrease the number of $p60_{217-225}$ epitopes generated during in vivo LM infection of wild-type mice, causing the reduced $CD8^+$ T cell response to this epitope. In this case, in vitro peptide quantitation experiments showing more $p60_{217-225}$ than LLO_{91-99} epitope after LM infection (*24*) may reflect the situation that occurs in vivo in GKO mice. This issue can be addressed by quantitation of peptides after infection of wild-type and IFN-γ–deficient mice.

Currently, little is known regarding the regulation of the death phase of Ag-specific $CD8^+$ T cells (*27*). Recent studies with LCMV infection demonstrate normal death of Ag-specific $CD8^+$ T cells in the absence of TNF receptor 1 (TNFRI) and CD95 (*28*, *29*), receptors that are critical for the phenomenon of activation-induced cell death. Two recent studies suggest that IFN-γ regulates apoptosis of activated $CD4^+$ T cells during *M. tuberculosis* infection or in the development of experimental autoimmune encephalitis (EAE) (*30*, *31*). IFN-γ could regulate the death phase of Ag-specific $CD8^+$ T cells directly; by controlling the expression of death factors, death receptors, or survival receptors such as IL-15R (*32*); or by sensitizing cells to the signals delivered by these receptors. The existence of IFN-γ receptor knockout mice and the capacity to identify and purify Ag-specific $CD8^+$ T cells via MHC class I tetramer technology should facilitate the testing of these hypotheses.

Alternatively, IFN-γ could indirectly regulate the death phase of $CD8^+$ T cell homeostasis. Recent studies reveal that naïve but not memory $CD8^+$ T cells require self-peptide–MHC complexes for homeostatic proliferation in lymphopenic hosts (*27*). Thus, it was suggested that the memory pool of $CD8^+$ T cells might be selected for the absence of low-affinity self-peptide–MHC interaction, so as to minimize the potential for inappropriate activation and autoimmune disease (*27*). In seeming contrast to this notion, analysis of TCR Vβ usage suggests that the repertoire of effector and memory $CD8^+$ T cells is similar (*33*, *34*). Studies with higher resolution may be required to address this issue. On the basis of our results, we speculate that IFN-γ could participate in selection of the memory pool by increasing the expression of self-peptide–MHC complexes, thus determining a threshold for survival that would prevent the inappropriate activation of memory cells during infection with unrelated pathogens. Consistent with this idea, preliminary studies reveal decreased MHC class I expression on spleen cells of LM infected GKO compared with wild-type mice (*7*). More detailed analyses are required to determine the relation between self-peptide–MHC class I expression and the death phase.

Our results demonstrate that perforin and IFN-γ not only contribute to pathogen clearance but also play major roles in $CD8^+$ T cell homeostasis that are distinct from their roles in control of infection. Because T cell memory is determined by the magnitude of expansion minus the death phase (*35*), our results may suggest strategies to enhance T cell memory in response to vaccination.

References and Notes

1. J. T. Harty *et al.*, *Annu. Rev. Immunol.* **18**, 275 (2000).
2. M. Matloubian *et al.*, *J. Virol.* **73**, 2527 (1999).
3. R. A. Brundage *et al.*, *Proc. Natl. Acad. Sci. U.S.A.* **90**, 11890 (1993).
4. J. T. Harty, M. J. Bevan, *Immunity* **3**, 109 (1995).
5. V. P. Badovinac, J. T. Harty, *J. Immunol. Meth.* **238**, 107 (2000).
6. M. K. Slifka, J. L. Whitton, *J. Immunol.* **164**, 208 (2000).
7. V. P. Badovinac, J. T. Harty, unpublished data.
8. S. Vijh, E. G. Pamer, *J. Immunol.* **158**, 3366 (1997).
9. D. H. Busch *et al.*, *Immunity* **8**, 353 (1998).
10. H. Shen *et al.*, *Cell* **92**, 535 (1998).
11. V. P. Badovinac, J. T. Harty, *J. Immunol.* **164**, 6444 (2000).
12. Web figures 1 and 2 are available at *Science* Online at www.sciencemag.org/cgi/content/full/290/5495/1354/DC1.
13. D. Kagi *et al.*, *Annu. Rev. Immunol.* **14**, 207 (1996).
14. A. Gallimore *et al.*, *J. Exp. Med* **187**, 1383 (1998).
15. D. W. White *et al.*, *J. Immunol.* **162**, 890 (1999).
16. K. Fruh, Y. Yang, *Curr. Opin. Immunol.* **11**, 76 (1999).
17. C. A. Nacy *et al.*, *Adv. Exp. Med. Biol.* **239**, 1 (1988).
18. K. Murali-Krishna *et al.*, *Immunity* **8**, 177 (1998).
19. A. Tishon *et al.*, *Virology* **212**, 244 (1995).
20. K. Schwarz *et al.*, *J. Immunol.* **165**, 768 (2000).
21. S. Sad *et al.*, *J. Exp. Med.* **184**, 1543 (1996).
22. P. Klenerman, R. M. Zinkernagel, *Nature* **394**, 482 (1998).
23. J. W. Yewdell, J. R. Bennink, *Annu. Rev. Immunol.* **17**, 51 (1999).
24. M. S. Villanueva *et al.*, *Immunity* **1**, 479 (1994).
25. D. H. Busch, E. G. Pamer, *J. Immunol.* **160**, 4441 (1998).
26. S. Vijh *et al.*, *J. Immunol.* **160**, 3971 (1998).
27. A. W. Goldrath, M. J. Bevan, *Nature* **402**, 255 (1999).
28. L. T. Nguyen *et al.*, *Eur. J. Immunol.* **30**, 683 (2000).
29. A. Reich *et al.*, *Eur. J. Immunol.* **30**, 678 (2000).
30. C. Q. Chu *et al.*, *J. Exp. Med.* **192**, 123 (2000).
31. D. K. Dalton *et al.*, *J. Exp. Med.* **192**, 117 (2000).
32. P. Marrack *et al.*, *Nature Immunol.* **1**, 107 (2000).
33. D. J. Sourdive *et al.*, *J. Exp. Med.* **188**, 71 (1998).
34. D. H. Busch, E. G. Pamer, *J. Exp. Med.* **189**, 701 (1999).
35. R. Ahmed, D. Gray, *Science* **272**, 54 (1996).
36. K. Inaba *et al.*, *J. Exp. Med.* **176**, 1693 (1992).
37. Attenuated LM strain DP-L1942 (ActA-deficient) (*3*) was prepared for injection and colony forming units (CFU) per spleen or per grams of liver were determined as previously described (*4*).
38. The magnitude of the epitope-specific $CD8^+$ T cell response was determined by ICS for TNF, IFN-γ, or MHC class I tetramer staining as previously described (*5*, *11*, *15*). For ICS, the percent of TNF^+ or IFN-γ^+ $CD8^+$ T cells in the unstimulated sample for each mouse was subtracted from the peptide stimulated value to determine the frequency of Ag-specific $CD8^+$ T cells. Total number of epitope-specific $CD8^+$ cells per spleen was calculated from this frequency, the percent of $CD8^+$ T cells in each sample, and total number of cells per spleen.
39. E. G. Pamer *et al.*, *Nature* **353**, 852 (1991).
40. E. G. Pamer *J. Immunol.* **152**, 686 (1994).
41. BALB/c bone marrow–derived dendritic cells, prepared by incubation for 6 days in granulocyte-macrophage colony-stimulating factor (GM-CSF) + interleukin-4 (IL-4) (*36*) were matured by incubation with lipopolysaccharide (50 ng/ml) for 48 hours. LLO_{91-99} and $OVA_{323-336}$ peptides (1 μM, final concentration) were added for the last 24 hours of culture.

42. We thank L. Gorton and G. Corbin for excellent technical assistance, J. Mahoney and D. Bonthius for assistance with LCMV titrations, the National Institute of Allergy and Infectious Diseases MHC Tetramer Core Facility for MHC Class I tetramers, and S. Perlman and T. Waldschmidt for critical review of the manuscript. Supported by NIH grants AI36864, AI42767, T32AI07511, and T32AI07260.

24 July 2000; accepted 17 October 2000